Biochimica et Biophysica Acta 896 (1987) 214–223
Elsevier

BBA 73198

Passive electrical properties of the membrane and cytoplasm of cultured rat basophil leukemia cells. II. Effects of osmotic perturbation

A. Irimajiri, K. Asami *, T. Ichinowatari and Y. Kinoshita

Department of Physiology, Kochi Medical School, Nankoku, Kochi 781-51 (Japan)

(Received 18 July 1986)

Key words: Dielectric dispersion; Membrane capacity; Conductivity, intracellular; Surface morphology; Anisosmotic challenge; Cell volume; Leukemia; (Rat basophil leukemia cell)

The effects of osmotic perturbation on the dielectric behavior of cultured rat basophilic leukemia (RBL-1) cells were examined. Cells exposed to osmolalities (π) of 145–650 mosmolal showed dielectric dispersions of the following characteristics: (1) Permittivity increment $\Delta\varepsilon(=\varepsilon_l-\varepsilon_h$ where ε_l and ε_h refer to the low- and high-frequency limit values) for a fixed volume concentration increased with π; (2) gross permittivity behavior was apparently of a typical Cole-Cole type; however, (3) frequency dependence of conductivity was undulant and could be simulated by a superposition of two separate Cole-Cole type dispersions; (4) separation of these subdispersions along the frequency axis was an increasing function of π, and so was conductivity increment in the high-frequency region. As examined by light microscopy, the cells were spherical in spite of imposed anisotonic stresses and behaved as osmometers at 200–410 mosmolal. When normalized by dividing by number (not volume) concentration, $\Delta\varepsilon$ remained relatively constant irrespective of π. Apparent membrane capacities (C_m), analyzed by applying a single-shell model, increased systematically from a hypotonic value of approx. 1 $\mu F/cm^2$ up to 5 $\mu F/cm^2$ at 650 mosmolal. This increase was interpreted as due to increased cellular 'surface/volume' ratios that were confirmed by scanning electron microscopy. Cole-Cole's β parameter, which culminated around 0.9 for isotonic cells and declined to approx. 0.8 for anisotonic cells, did not parallel the broadening of cell volume distribution but appeared to reflect changes in the intracellular conductivity caused by the anisotonic challenge. The results indicate that the dispersion method can probe changes in surface morphology as well as subcellular organelles' constitution of living cells.

Introduction

In the preceding paper [1] (hereafter, Paper I) we have described the dielectric behavior of a cultured cell line (RBL-1) reporting that the cells in a physiological medium display a conspicuous 'two-step' frequency dependence when measured over a wide frequency range. Such an apparently composite 'two-step' dispersion was new to the authors' knowledge and differed from any of the dispersion patterns so far reported for red blood [2–4], ascites tumor [5] and lymphoma [6,7] cells.

To further characterize the cellular dielectric behavior, it seems pertinent to examine the effects of osmotic perturbation, since, by this maneuver, parameters such as cytosolic conductivity and rel-

* Present address: Institute for Chemical Research, Kyoto University, Uji, Kyoto 611, Japan.

Correspondence: A. Irimajiri, Department of Physiology, Kochi Medical School, Okohcho, Nankoku, Kochi 781-51, Japan.

ative organellar volume would undergo a forced variation. For instance, a lowered or an elevated internal conductivity would result from hypo- or hypertonic treatment, respectively. In addition, if the anisosmotic challenge is limited within a reasonable range, the membrane-related parameters, such as permittivity, conductivity and thickness, are all expected to survive environmental changes elicited by redistribution of cell water, and so to remain relatively unaffected once osmotic equilibrium is reestablished across the plasma membrane. These expectations underlie the rationale of the present study.

We now describe a cellular response to anisotonic milieus, particularly in terms of the cells' dielectric behavior as correlated with surface morphological changes. Analyses of membrane capacity and interior conductivity revealed some initially unexpected but reasonable aspects of alterations in the electrical and anatomical constitution of living cells.

Materials and Methods

Cell culture, morphometry, viability test and dielectric measurements were all performed as described in Paper I. Cells of a single batch were divided into four or five aliquots, diluted with about 100 volumes of the respective test media and equilibrated for 15 min at room temperature before they were subjected to dielectric measurements. The waiting time of 15 min was chosen after a check for regulatory volume changes [8,9] that were completed within 10 min under the present experimental condition. Dielectric measurements were done at 30 ± 0.1°C.

Test solutions of graded osmolalities adjusted with mannitol had an identical ionic strength; they contained a half-normal concentration of culture medium (RPMI 1640) and 20 mM Hepes-Tris buffer (pH 7.4). In some experiments the final conductivities, not ionic strengths, were matched for each pair of test media by adjusting their NaCl concentrations.

For scanning electron microscopy (SEM), the cells sampled from suspensions for dielectric measurements were immobilized onto cover slips precoated with poly(L-lysine) [10] and fixed at 4°C overnight in phosphate-buffered 1% (w/v) glutaraldehyde fixatives having total osmolalities equal to those of the media used for the dielectric measurements. Specifically, the most hypotonic fixative (145 mosmolal) contained 1% (w/v) glutaraldehyde and 15 mM sodium phosphate buffer (pH 7.4), and the most hypertonic (650 mosmolal) contained 1% (w/v) glutaraldehyde, 300 mM mannitol and 100 mM phosphate buffer (pH 7.4); intermediate ones were prepared by adjusting their mannitol and buffer concentrations while maintaining both their aldehyde concentration and pH constant at 1% and 7.4, respectively. The cells were postfixed in 1% (w/v) osmium tetroxide/100 mM phosphate buffer for 1 h at 4°C, dehydrated in an ethanol series, critical-point dried using CO_2, sputter coated, and then examined under a Hitachi S-450 scanning electron microscope.

Results

Dielectric behavior

Fig. 1 shows dispersion curves for the cells incubated in various osmolalities. Here, the data have been plotted after normalization with respect to both the dispersion magnitude ($\Delta\varepsilon = \varepsilon_l - \varepsilon_h$ or $\Delta\kappa = \kappa_{10f_c} - \kappa_l$) and the center frequency (f_c) because these parameters for individual dispersions were variable depending on the volume fraction and medium species employed (Table I). As seen in Fig. 1A, the normalized permittivity dispersions resembled each other in their overall shape, though there were subtle differences in slope at around $f = f_c$, and concluded within about three decades of frequencies spanning across the f_c values. By contrast, the conductivity dispersions (Fig. 1B) did not level off but rather tended to increase with the applied frequency, giving rise to a complicated frequency dependence. Moreover, the increments in κ per decade increase of frequency were even steeper in the high-frequency region for the cells having experienced higher osmolalities.

Fig. 2 shows the complex plane plots. It is to be noticed that the loci in Fig. 2A, all apparently of a simple circular-arc type, were least depressed for the isotonic (271 osmolal) cells and became more depressed as the medium was made more hypo- or hypertonic. Values of the parameters, $\Delta\varepsilon$, f_c, and β, each from the complex plane plot, are listed in Table I. In the complex conductivity

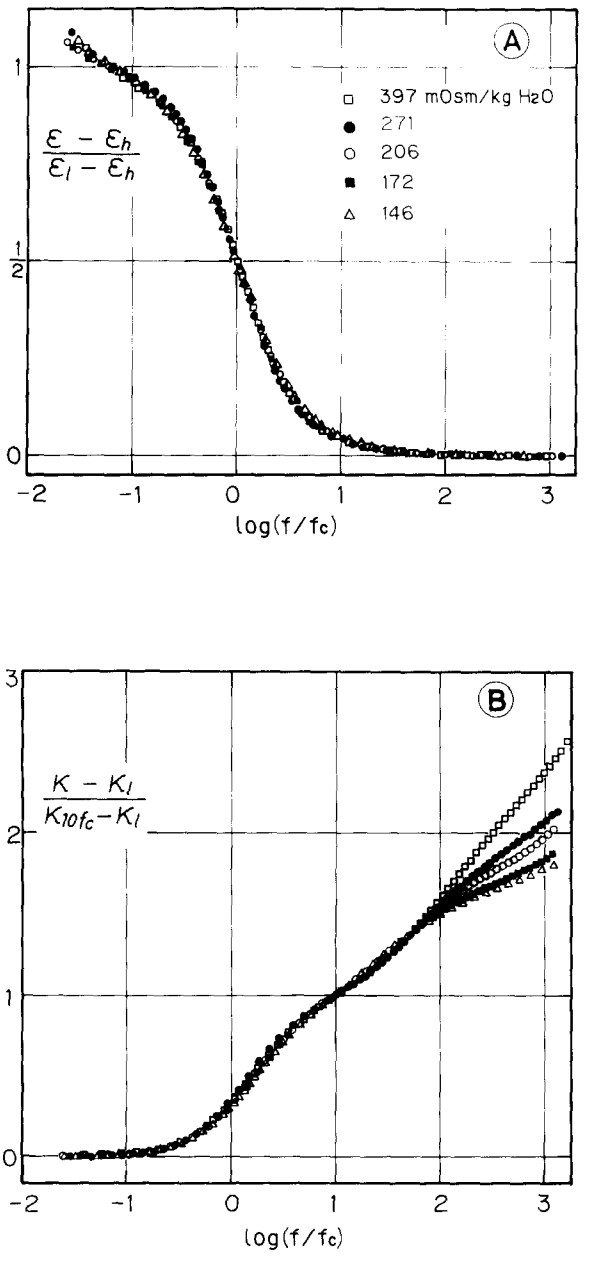

Fig. 1. Dielectric dispersion curves obtained using a single batch of cultured cells that were divided into aliquots and subjected to different osmolalities. Abscissae: Log of frequency relative to characteristic frequency f_c. Ordinates: (A) Normalized permittivity increment, $(\varepsilon - \varepsilon_h)/(\varepsilon_l - \varepsilon_h)$, where ε_l and ε_h are the limiting values of ε extrapolated (as in Fig. 2A) to low and high frequencies, respectively; (B) normalized conductivity increment, $(\kappa - \kappa_l)/(\kappa_{10f_c} - \kappa_l)$, where κ_l and κ_{10f_c} are conductivities at the low-frequency limit and at the frequency one decade above f_c.

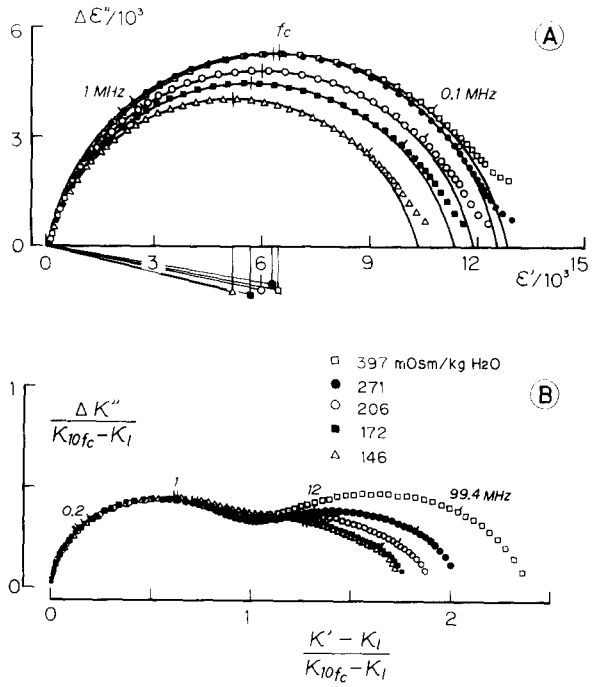

Fig. 2. Complex relative permittivity (A) and complex conductivity (B) plane plots of data in Fig. 1. In (A), points below the real axis indicate centers for the circular arcs; vertical lines atop of the circular loci, characteristic frequencies f_c.

diagram (Fig. 2B), all the traces gave a bimodal pattern indicative of the involvement of at least two subdispersions, as already pointed out in Paper I. Furthermore, with increasing osmolality, dispersion 2 at higher frequencies augmented its proportion to dispersion 1 which remained relatively invariant in the submegahertz region.

Fig. 3 illustrates measurements in which the cells were equilibrated with two anisosmotic but isoconductive media and suspended in the respective media such that the resultant suspensions shared the same level of conductivity at low enough frequencies. This maneuver was intended to make their volume concentrations matched as closely as possible, thereby facilitating a direct comparison of the two dispersion curves free from the effect of unbalanced volume fractions. It is clear from Fig. 3 that (1) gross permittivity increment $\Delta\varepsilon$ is much greater for the cells exposed to hypertonicity (413 mosmolal) than for the cells rendered swollen by a hypotonic (172 mosmolal) treatment, (2) both dispersion curves can be simulated by the two-term

TABLE I

DIELECTRIC PARAMETERS FOR DATA IN Figs. 1 AND 2

Medium			Suspension					
π (mosmolal)	ε_a	κ_a (mS/cm)	κ_1 (mS/cm)	Φ [a]	$\Delta\varepsilon$ ($\times 10^{-4}$)	f_c (kHz)	θ (deg)	β [b]
397	80.9	6.92	2.30	0.520	1.281	317	79.4	0.882
271	81.0	7.64	2.34	0.545	1.235	379	80.5	0.894
206	81.6	7.43	1.69	0.628	1.177	420	78.6	0.873
172	81.4	7.59	1.67	0.636	1.124	426	76.6	0.851
146	81.2	7.48	2.06	0.577	1.016	419	76.2	0.847

[a] Volume fraction, calculated from $\Phi = 1 - (\kappa_1/\kappa_a)^{2/3}$ [17].
[b] Cole-Cole's parameter, calculated from $\beta = \theta/90$ [12].

TABLE II

DIELECTRIC PARAMETERS DETERMINED BY SIMULATION IN Fig. 3

Suspension	π (mosmolal)	κ_1 (mS/cm)	ε_h	Dispersion 1			Dispersion 2		
				$\Delta\varepsilon_1$ ($\times 10^{-3}$)	f_{c1} (kHz)	β_1	$\Delta\varepsilon_2$	f_{c2} (MHz)	β_2
A	172	4.53	69	7.10	389	0.910	70	9.4	0.990
B	413	4.60	61	11.30	276	0.887	58	25	0.868

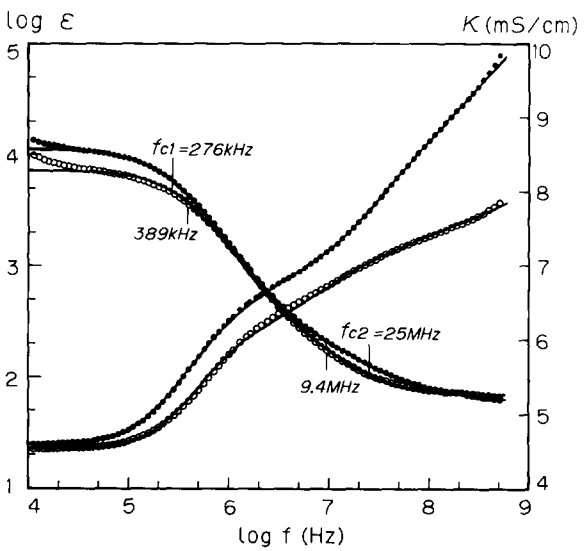

Fig. 3. Comparison of the osmotic effects on the dielectric behavior of cells in two media of the same conductivity (κ_a = 7.608 mS/cm at 30°C) and of different osmolalities: π = 413 (●) and 172 (○) mosmolal. Note that the low-frequency conductivities for the two suspensions were made close to each other by adjusting their volume fractions.

Cole-Cole equation [1] with parameters listed in Table II, and (3) raised tonicity shifts dispersion 1 toward the lower-frequency side and dispersion 2 toward the higher-frequency side.

Cell morphology

In an attempt to correlate the dielectric behavior with cell morphology, we measured the diameter (D) for unfixed cells as a function of medium osmolality. As the cells were spherical within the test range of osmolality, we calculated an average volume ($\bar{V}$) for a given specimen and a volume-averaged diameter ($\bar{D}$) as $(6\bar{V}/\pi)^{1/3}$. For various osmolalities the size distribution widths were all alike, whereas the $\bar{D}$ varied rather systematically with π. A linear osmometric behavior obeying the Boyle-van't Hoff rule was confirmed over 200–410 mosmolal; outside of this range, however, some deviations therefrom. An osmotic dead space was estimated to be somewhere between 5 and 50% relative to the isotonic cell volume of approx. 1.5 pl.

Fig. 4 illustrates changes in surface morphology

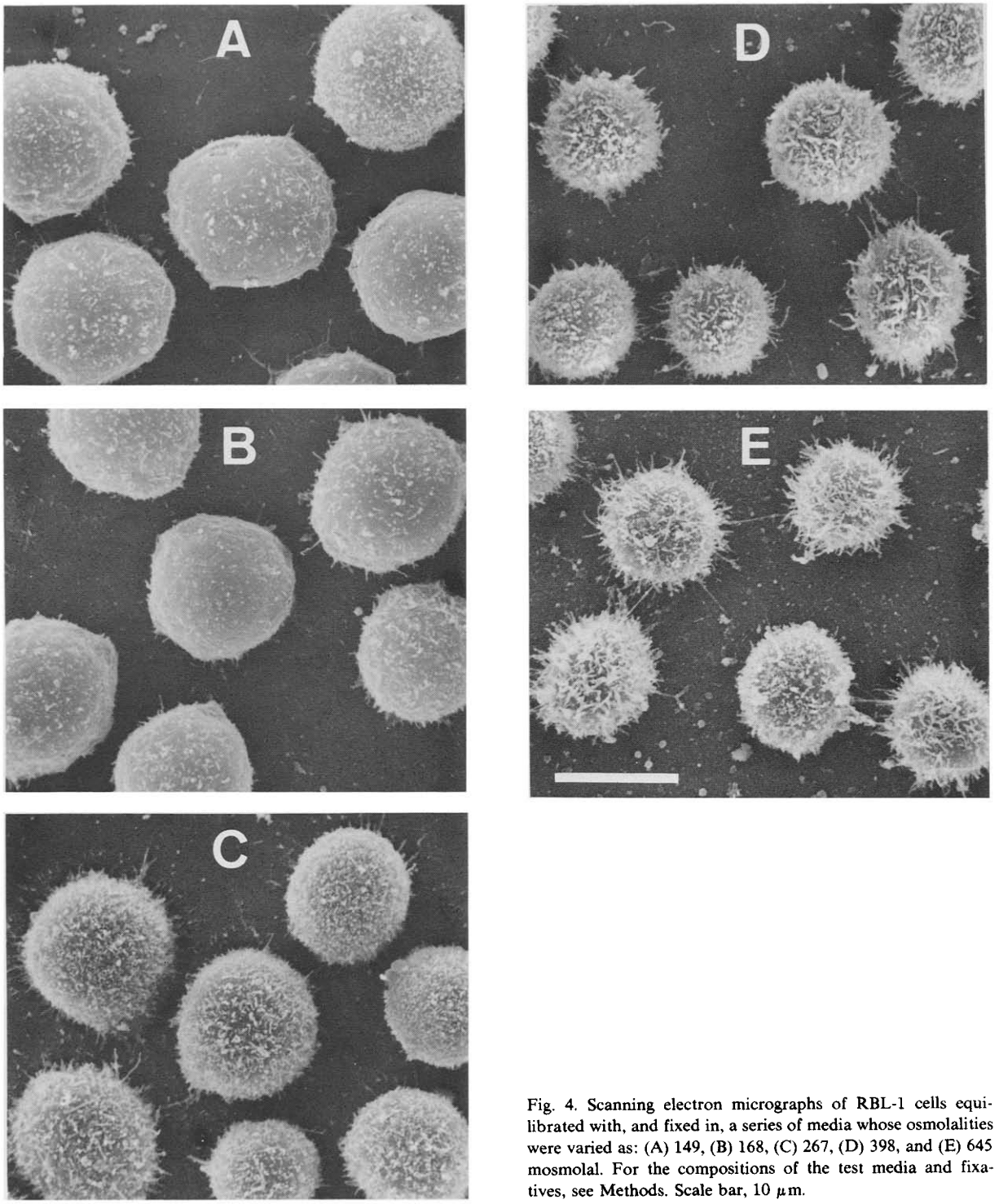

Fig. 4. Scanning electron micrographs of RBL-1 cells equilibrated with, and fixed in, a series of media whose osmolalities were varied as: (A) 149, (B) 168, (C) 267, (D) 398, and (E) 645 mosmolal. For the compositions of the test media and fixatives, see Methods. Scale bar, 10 μm.

for the cells, perturbed osmotically. In this experiment, care was taken that the cells were fixed isosmotically with the preincubation media. The scanning electron microscopy images show that the cells were spheroidal and villated in such a fashion as to make their microvilli thicker and more elongated with advancement of cell shrinkage. How faithfully the SEM procedure employed could reproduce the real surface morphology of the intact cells remains an open question, however. In fact, many causes of artifacts have been reported for the SEM technique especially when dealing with free-floating mammalian cells (for a review, see for example Ref. 11). Hence, the osmotically-induced surface changes described above should not be given full credit, particularly to their quantitative aspect, and could therefore be reinforced with supporting evidence from different approaches such as the dielectric analysis of living cells.

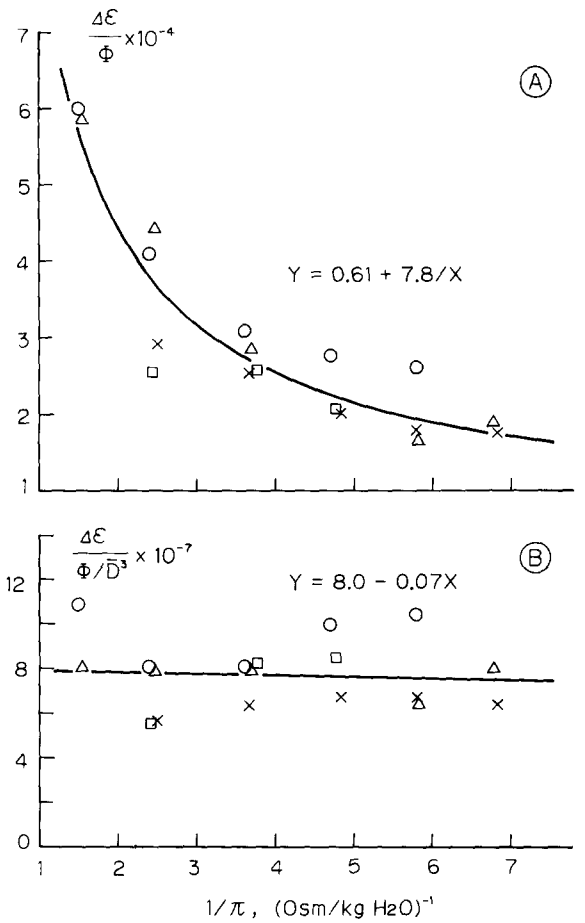

Fig. 5. Plots of $\Delta\varepsilon/\Phi$ and $\Delta\varepsilon/(\Phi/\bar{D}^3)$ against $1/\pi$, where $\Delta\varepsilon$ denotes permittivity increment, Φ volume fraction and $\bar{D}$ mean cell diameter in μm. The data are from four separate experiments as represented by different symbols. Solid lines indicate the regression results: (A) hyperbolic ($r^2 = 0.862$) and (B) linear ($r^2 = 0.006$).

Comparison of the dielectric and morphological parameters

Fig. 5 compares the permittivity increments as a function of reciprocal osmolality in the following two ways. In Fig. 5A, the $\Delta\varepsilon$ has been divided by volume fraction Φ for the purpose of eliminating the effect of scattered volume concentrations. The result shows a hyperbolic dependence of $\Delta\varepsilon/\Phi$ upon $1/\pi$. In contrast, when normalized by dividing by $\Phi/\bar{D}^3$, a parameter proportional to cell number concentration, the reduced increment $\Delta\varepsilon/(\Phi/\bar{D}^3)$ is essentially independent of π (Fig. 5B), a fact indicating that the suspension of cells exposed to anisotonicities, despite accompanying forced changes in cell volume, does maintain its

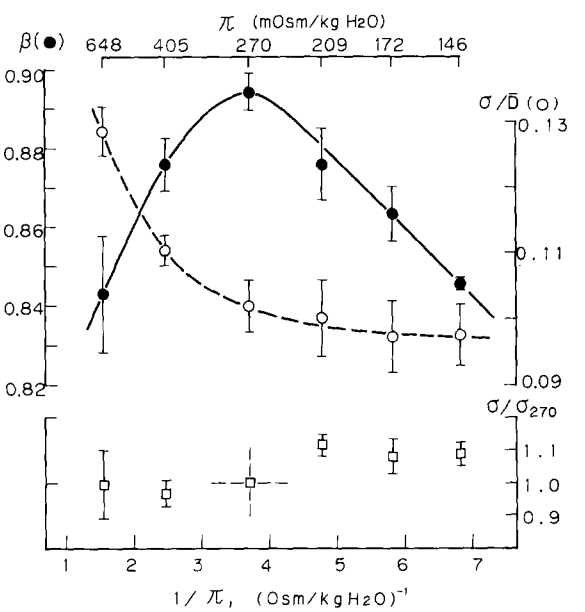

Fig. 6. Comparison of the osmolality dependence of Cole-Cole's parameter (β) and that of cell size distribution expressed as $\sigma/\bar{D}$ or σ/σ_{270}, where $\bar{D}$ is cell diameter, σ is standard deviation (S.D.) of D, and σ_{270} is S.D. for 270 mosmolal. Each point represents mean $\pm$ S.E. of 2–4 separate determinations. The lines were fitted by eye.

original isotonic magnitude of $\Delta\varepsilon$ so long as the cell 'number' concentration is kept constant.

Fig. 6 compares the osmolality dependence of β, a measure for distributed relaxation times [12], with that of size heterogeneity expressed as 'coefficient of variation' ($\sigma/\bar{D}$) or 'relative variation' (σ/σ_{270}). Clearly, there is no simple parallelism between the β parameter and the size distribution indices as represented by the standard deviation σ. Hence, the dispersion broadening in terms of the β-values of 0.8–0.9 must have been brought about largerly through a certain mechanism other than heterogeneity in cell size.

Discussion

The present data have confirmed our finding [1] that the RBL-1 cell shows a 'bimodal' dispersion pattern, which is simulated by a superposition of two Cole-Cole type relaxations, the second one being most probably due to intracellular membranal organelles. Quite unexpectedly, however, the permittivity increment $\Delta\varepsilon$ was strongly dependent on medium osmolality, and hence on cell volume, but rather insensitive to volume fraction itself when the cell number concentration was taken as a normalizing factor. In addition, the conductivity behavior also changed with osmolality, indicating that alterations in the extracellular osmolality not only perturb the cell surface structure but affect the state of cell interior in a rather complicated fashion. In the discussion below, we shall focus on the possible relationship between the changes in the passive electrical parameters and those in the morphological ones.

Dielectric capacity of the cell membrane

In general, the dispersion magnitude $\Delta\varepsilon$ for a fixed Φ-value is an increasing function of cell size (D), insofar as we assume a single-shell model in which the specific membrane capacity (C_m) is meant to be independent of D [13,14]. If this would also apply to the osmotic cell volume changes, then the $\Delta\varepsilon/\Phi$ should have been an increasing function of $1/\pi$ in view of the observed osmometric behavior. However, the result obtained was not expected; instead, it gave a hyperbolically declining function (Fig. 5A). This finding favors the idea that the C_m for the living cells may vary several-fold in response to an osmotic perturbation. In fact, with increase in π, the C_m calculated using a conventional shell model (Eqns. 6 and 8, Ref. 1) increased over 4 μF/cm^2 (cf. Fig. 7), yielding a curve similar to Fig. 5A. It should be here noted that these values for C_m are apparent in the sense that they did not necessarily represent the 'true' C_m, or the capacity per unit area of a flat membrane, because the actual cell surface was rather heavily villated (Fig. 4), and hence, far from being smooth enough to satisfy the premise underlying the shell model employed here. Now a question arises: What does the apparent C_m mean?

The membrane capacity C_m as a measure for 'microvillation'

The reduced increment, $\Delta\varepsilon/(\Phi/\bar{D}^3)$, was almost insensitive to change in π (Fig. 5B). Based on this fact, we will derive an empirical equation that relates the apparent C_m to the degree of microvillation on cell surface. By assuming a linear relationship between $\Delta\varepsilon$ and $\Phi R C_m$ [13,14], with R for mean cell radius, we have a simple proportionality

$$\Delta\varepsilon/(\Phi/R^3) \propto C_m R^4 \tag{1}$$

where the denominator is again a parameter for the cell number concentration. So that, if the left-hand side of Relation 1 does not change appreciably with change in R, we obtain

$$C_m R^4 = \text{constant} \tag{2}$$

Eqn. 2 claims that the C_m vs. R, plotted double-logarithmically, should yield a straight line of slope -4, which has been verified for the present data (Fig. 7). Now, suppose a spherical cell rendered critically swollen to have a smooth surface of area $4\pi R_0^2$ with its specific membrane capacity C_{m0} undergoes osmotic shrinkage towards a new state where the cell's equivalent radius is reduced to R accompanied by an increase in its 'apparent' membrane capacity to C_m. Then, immediately from Eqn. 2,

$$C_m/C_{m0} = (R_0/R)^4 \tag{3}$$

Next, define the 'microvillosity' μ as a measure for the density of microvilli formed on the cell

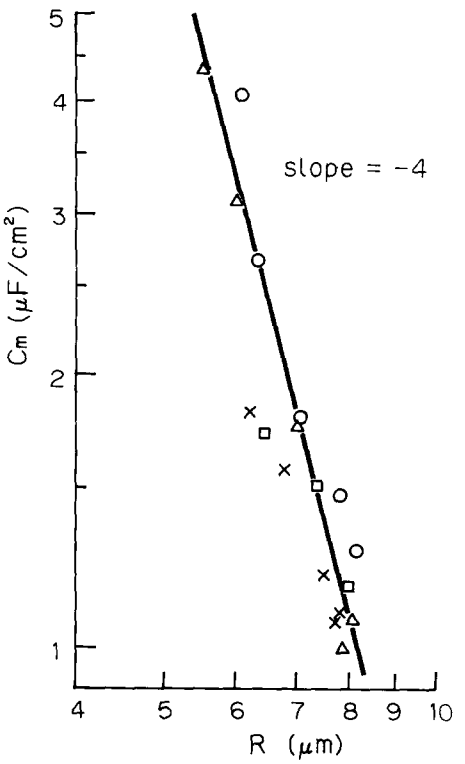

Fig. 7. 'Apparent' membrane capacity (C_m) vs. cell radius (R), plotted double logarithmically. Different symbols refer to four separate experiments. The line was drawn by eye.

surface such that

$$\mu = S_0/S = (R_0/R)^2 \tag{4}$$

where S_0 and S are the initial (total) surface and the final equivalent-spherical (not total) areas, respectively. Combining Eqns. 3 and 4, we have

$$\mu = (C_m/C_{m0})^{1/2} \tag{5}$$

By applying Eqn. 5 to the C_m data presented, the degree of microvillation for the most hypertonic cells is estimated to have doubled that for the most hypotonic cells, or μ (at 645 mosmolal)/μ (at 145 mosmolal) $\simeq$ 2, a value not so unrealistic in light of the surface changes seen from the scanning electron microscopy images (Fig. 4).

The estimation of μ described above has been based on two assumptions. First, $\Delta\varepsilon$ is linearly dependent on either of Φ, R or C_m. Strictly, however, the linear dependence on Φ holds only approximately and theory shows that the Φ should be replaced by $\Phi/(1+\Phi/2)^2$ even in dilute suspensions [13]. Therefore, Eqn. 5 is of a limited applicability especially when dealing with relatively concentrated suspensions as used in the present study. The second assumption made is conservation of the total membrane area against the changes of cell volume. To a first approximation, this seems reasonable in that a massive membrane incorporation into, or depletion from, the cell surface would not have occurred in 10 min or so within the test range of osmolality. Neither likely is the possibility that the imposed hypoosmotic stress caused membrane distention leading to a substantial (e.g., 2-fold) increase in the total surface area accompanied by a decrease in the membrane thickness. If this had ever been the case, the most hypotonic cells should have simultaneously had a C_m greater than the isotonic cells and a smooth (non-villated) appearance; all the experimental results point to the contrary.

Gross conductivity of the cell interior

Analysis by the single-shell model, in which the cell interior is simply regarded as a homogeneous phase, informs us of an equivalent homogeneous ('gross') conductivity for that phase, denoted here by $\bar{\kappa}_i$. At isotonicity, the $\bar{\kappa}_i$ values collected from four separate experiments were about one-half of the medium conductivity (κ_a) with a ratio $\bar{\kappa}_i/\kappa_a$ (or relative $\bar{\kappa}_i$) ranging from 0.45 to 0.55. As the osmolality departed away from isotonicity, the relative $\bar{\kappa}_i$ became lower than that for the isotonic cells (Fig. 8). A qualitative interpretation of this finding, though tentative at present, will be given below.

Suppose the whole intracellular space as a secondary suspension comprised of aqueous cytosol (the continuous phase) of conductivity κ_c and a mass of membrane-bounded particles (the suspended phase) that occupy part of the space to a volume fraction ϕ. Since the organellar membranes in general can safely be assumed to be several orders of magnitude less conductive than the cytosolic phase (cf. Refs. 6 and 15 for nuclear and mitochondrial membranes, respectively), the following relation is expected to apply to the subcellular secondary suspensions [16,17]

$$\bar{\kappa}_i/\kappa_c = (1-\phi)^{3/2} \tag{6}$$

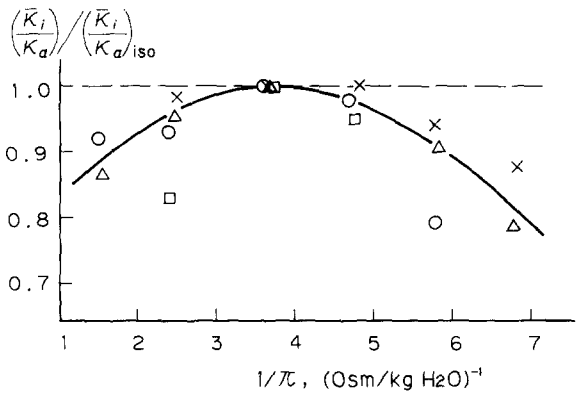

Fig. 8. Intra-to-extracellular conductivity ratio ($\bar{\kappa}_i/\kappa_a$) as a function of $1/\pi$. Values of $(\bar{\kappa}_i/\kappa_a)_{iso}$, which refers to the ratio for isotonic specimens, are as: 0.547 (○), 0.538 (△), 0.502 (□) and 0.448 (×). The line was fitted by eye.

which may be further rewritten as

$$(\bar{\kappa}_i/\kappa_a)(\kappa_a/\kappa_c) = (1-\phi)^{3/2} \tag{7}$$

Eqn. 7 implies that, given one of the two parameters (κ_a/κ_c and ϕ), the other can be estimated experimentally since the $\bar{\kappa}_i/\kappa_a$ is observable as noted above.

One inference from Eqn. 7 on the osmotic behavior of ϕ is schematically illustrated in Fig. 9. Here, the basic assumption to start with is an inverse relationship between κ_c and $1/\pi$ as a result of redistribution of cell water, and hence, a monotonous increase of κ_a/κ_c with increase in $1/\pi$. Taking into account the observed 'bell-shaped' behavior of $\bar{\kappa}_i/\kappa_a$ (Fig. 8), the term $(1-\phi)^{3/2}$ must be an increasing function of $1/\pi$ at least for the cells exposed to hypertonicity. In the hypotonic region, however, the same term may well tend to either increase or decrease or stay near the isotonic level, depending on the cells' specific conditions involved. Thus, a likely conjecture would be such that the cells swell in response to external hypotonicity accompanying a roughly proportional increase in their organellar volume, whereas the cells subject to hypertonicity rather resist a drastic volume reduction of the organelles in situ, a sort of 'rectification' in the subcellular responses to osmotic perturbation.

It seems relevant to note that with the present cells the Cole-Cole parameter β also showed a

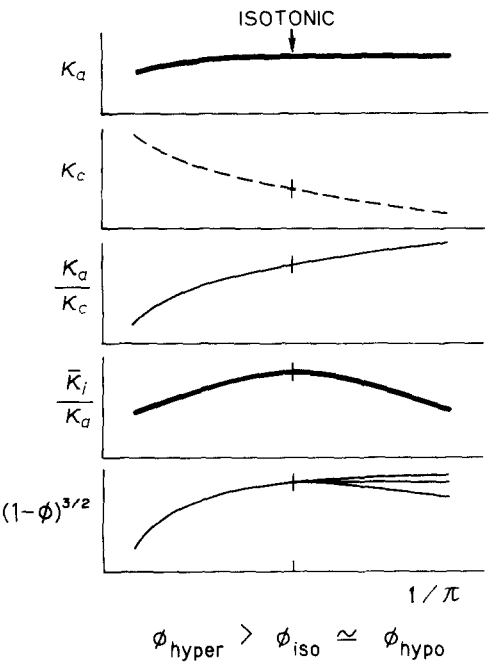

Fig. 9. Prediction of the effects of extracellular osmotic perturbation on the intracellular organellar volume. The volume fraction of membrane-covered organelles is denoted by ϕ; suffix to ϕ, hyper, iso or hypo, implies that the cells are subjected to hyper-, iso- or hypotonicity. ——— , observed; — — —, assumed; ———, predicted.

'bell-shape' dependence upon osmolality (Fig. 6). In view of the foregoing analysis of $\bar{\kappa}_i$, this could be an indication that individual cells perturbed with the same anisotonicity do not necessarily change their organellar volume in a coherent manner, thereby leaving a broader distribution of their ϕ values (and hence, of $\bar{\kappa}_i$ values) compared with the isotonic cells. In any case, whether or not our inference on the intracellular event following anisotonic challenge is likely awaits further studies with respect to the morphometry of cell organelles, which will be dealt with in Paper III.

Acknowledgments

We thank Dr. T. Suzaki for reading the manuscript and Mr. K. Yagui for assistance in electron microscopy. This work was supported in part by grants 56770052, 56870020 and 60770082 from The Ministry of Education, Science and Culture of Japan.

References

1 Irimajiri, A., Asami, K., Ichinowatari, T. and Kinoshita, Y. Biochim. Biophys. Acta (1987) Biochim. Biophys. Acta 896, 203–213
2 Pauly, H. and Schwan, H.P. (1966) Biophys. J. 6, 621–639
3 Jenin, P.C. and Schwan, H.P. (1980) Biophys. J. 30, 285–294
4 Asami, K., Hanai, T. and Koizumi, N. (1980) Jap. J. Appl. Phys. 19, 359–365
5 Pauly, H. (1963) Biophysik 1, 143–153
6 Irimajiri, A., Doida, Y., Hanai, T. and Inouye, A. (1978) J. Membrane Biol. 38, 209–232
7 Irimajiri, A., Hanai, T. and Inouye, A. (1979) J. Theor. Biol. 78, 251–269
8 Macknight, A.D.C. and Leaf, A. (1977) Physiol. Rev. 57, 510–573
9 Kregenow, F.M. (1981) Ann. Rev. Physiol. 43, 493–505
10 Tsutsui, K., Kumon, H., Ichikawa, H. and Tawara, J. (1976) J. Electron Microsc. 25, 163–168
11 Roath, S., Newell, D., Polliack, A., Alexander, E. and Lin, P.-S. (1978) Nature 273, 15–18
12 Cole, K.S. and Cole, R.H. (1941) J. Chem. Phys. 9, 341–351
13 Pauly, H. and Schwan, H.P. (1959) Z. Naturforsch. 14b, 125–131
14 Hanai, T., Koizumi, N. and Irimajiri, A. (1975) Biophys. Struct. Mech. 1, 285–294
15 Asami, K. and Irimajiri, A. (1984) Biochim. Biophys. Acta 778, 570–578
16 Hanai, T. (1960) Kolloid-Z. 171, 23–31
17 Irimajiri, A., Hanai, T. and Inouye, A. (1975) Experientia 31, 1373–1374